

**J. KRÁLIK**

# DETERMINISTIC AND PROBABILISTIC ANALYSIS OF DAMPING DEVICE RESISTANCE UNDER IMPACT LOADS FROM NUCLEAR FUEL CONTAINER DROP

**Juraj KRÁLIK**

email: juraj.kralik@stuba.sk  
Research fields: earthquake engineering, numerical mechanics, nonlinear mechanics, stochastic mechanics, and the safety and reliability of nuclear power plants

Department of Structural Mechanic,  
Faculty of Civil Engineering,  
Slovak University of Technology in Bratislava,  
Radlinského 11, 813 68, Bratislava, Slovakia.

## ABSTRACT

*This paper presents a deterministic and probabilistic solution of damping devices for the protection of the reinforced concrete structure of a nuclear power plant (NPP) from impact loads from a container of nuclear fuel of the type TK C30 drop. The finite element idealization of the building structure is used in space. The interaction soil-structure, as well as the fluid-structure of the deactivated basin is considered in space. A steel pipe damper system is proposed for the dissipation of the kinetic energy of the container in free fall. The Newmark integration method is used for the solution of the dynamic equations. The sensitivity and probabilistic analysis of the damping devices was realized using the AntHILL and ANSYS software.*

## KEY WORDS

- Impact,
- Damping device,
- Probability,
- Sensitivity
- Container drop,
- MONTE CARLO,
- SFEM,
- AntHILL,
- ANSYS

## 1. INTRODUCTION

The International Atomic Energy Agency (IAEA) initiated a program in 1990 to assist the countries of Eastern Europe and the Soviet Union in evaluating the safety of their first generation WWER-440/230 nuclear power plants. The main objectives of the program were: to identify major design and operational safety issues, to establish an international consensus on priorities for safety improvements, and to provide assistance in the review of the completeness and adequacy of safety improvement programs. The scope of the program was amended in 1992 to include RBMK, WWER-440 and WWER-1000 plants in operation and construction.

The program was complemented by national and regional technical cooperation projects. The results, recommendations and conclusions resulting from the IAEA program were intended only to assist

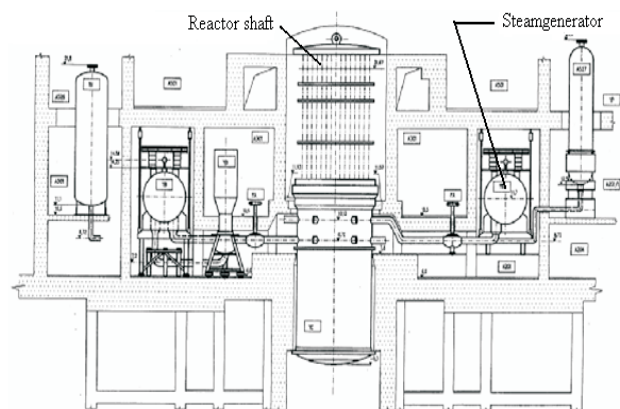


**Fig. 1** Scheme of a Nuclear Power Plant.

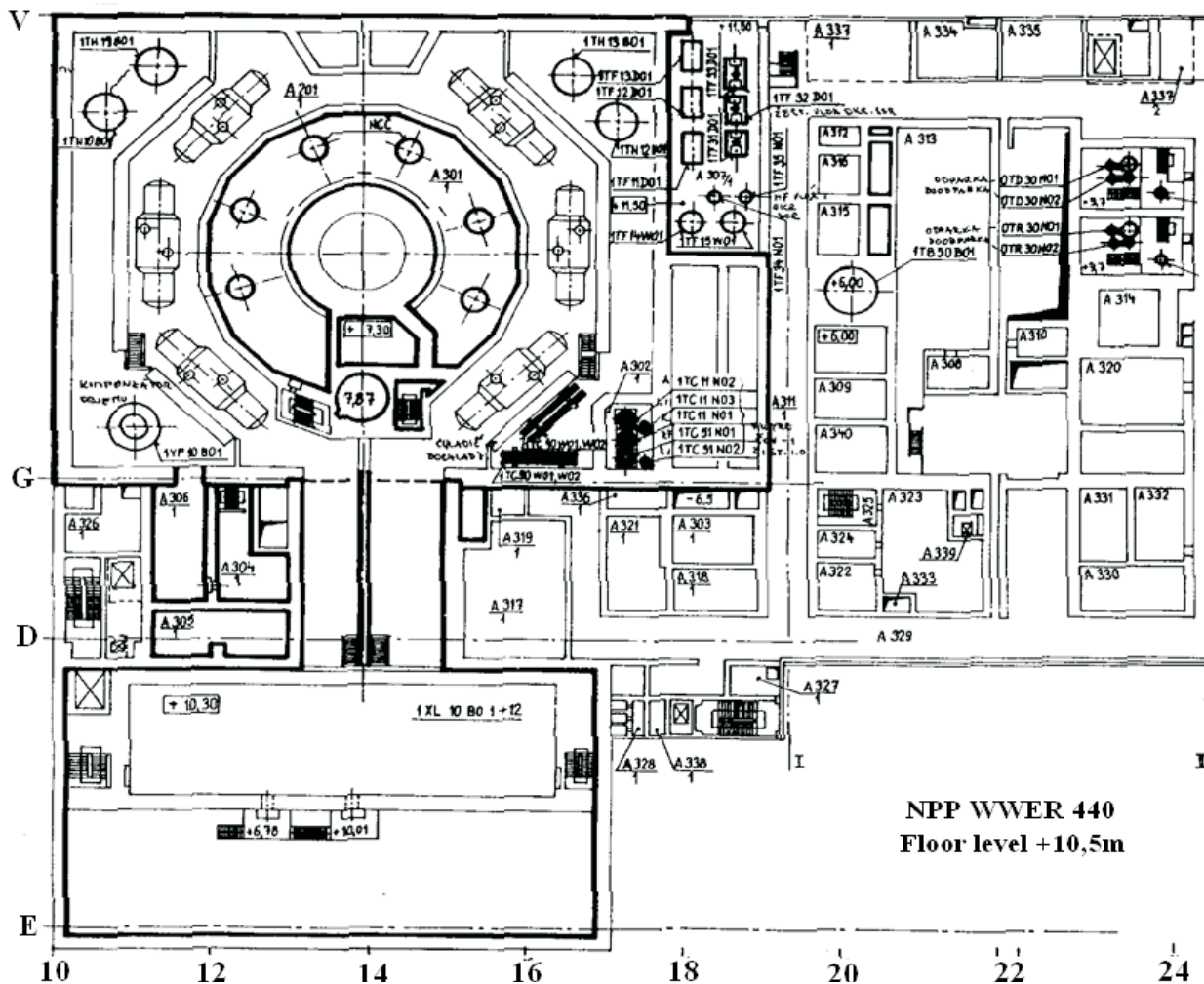
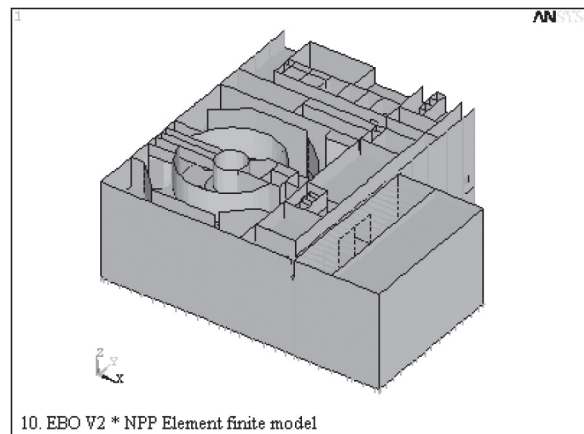
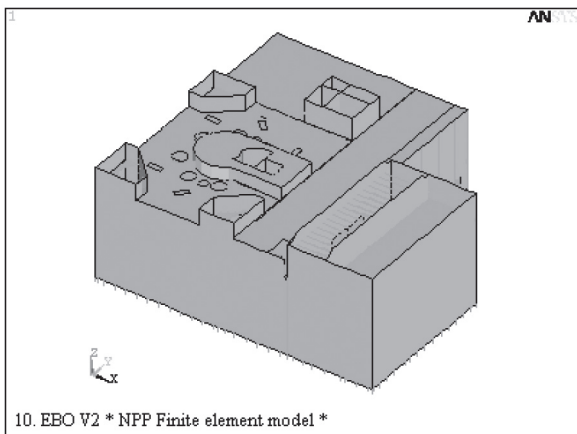


Fig. 2 Scheme of Nuclear Power Plant Floor level +10.5 m.

national decision makers who have to resolve responsibilities for the regulation and safe operation of their nuclear power plants. The Russian Federation's regulations as well as the IAEA NUSS Series documents, and rules, guidelines, safety standards and general review procedures practiced in Western countries as well as in the Russian Federation and Slovakia were compared by IAEA (1996). One significant accident is the possible drop of a container during the replacement of the nuclear fuel in the reactor shaft and the emergency basin. This accident can arise due to the failure of the crane hanger. It is necessary to remark that this operation is carried out during a technological pause. Hence, this accident does not affect the environs.

The reinforced concrete structure of the NPP containment can be penetrated as a consequence of the container's drop. All penetrations through the containment should meet the same design requirements as the containment structure itself. Bankash, M. Y. H. (1993), Cesnak, J., Králik, J. (2001), IAEA (1996) and Malý, et al. (2003). The containment should be protected against reaction forces stemming from pipe movements or accidental loads such as jet forces, pipe whip and missiles. According to the principles of the European Concrete Code ENV 1992, three types of load combinations can be considered. The first type of combination is that which corresponds to the serviceability limit state. The second type of combination is the fundamental ultimate limit





**Fig. 3 a, b** Calculation model of NPP building.

state and is used to verify the structural integrity with the normal safety factor on the load and on the material. It is used for primary and secondary ruptures, normal operating conditions and normal operating conditions in combination with the operating basis of an earthquake. The third type of combination is the accidental ultimate limit state. It is used to verify the structural integrity for an external hazard of low probability (airplane crash, SSE) and simultaneous LOCA and seismic events.

Cesnak, J. and Králik, J. (2001) considered one of the load cases presented, i.e., the impact loads according to the free fall of a container at the time of the exchange of nuclear fuels. The simulation of a reinforced concrete structure's behavior during an impact load is considered by Clough and Penzien (1993), Králik (1995, 2006, 2009), Kotrasová (2008) and Richart, et al. (1994), the interaction between a structure and the soil and the interaction between the structure and fluid in a deactivated basin, Bankash (1993), Králik and Cesnak (2001), Kanický and Salajka (1994), Kotrasová (2008), Malý, et al. (2003), Plocek, et al. (2007), Žmindák, et al. (2008).

Analyzing the reinforced concrete structure of the containment for different kind of loads was performed using the ANSYS software. The building of a power block was idealized with a discrete model, consisting of the solid elements (SOLID 45), shell elements (SHELL 43), beam elements (BEAM 4), linear actuator elements (LINK 11), mass elements (MASS 21), and solid fluid elements (FLUID 80). A finite element model was created from 20,840 elements and 15,600 nodes (see Fig. 3). A model is the best estimation of the behavior of a structural element (walls, plates, etc.) of a real NPP structure from the point of view of the geometric dimensions and material properties. The FEM model in Fig. 3 is very similar to the drawing in Figs.1 and 2. The possible point of the impact load is indicated by the arrows in Fig. 3b.

## 2. FORMULATION OF DYNAMIC EQUATIONS

The dynamic equation in time is obtained through a structure model with finite elements and with the approximation of a displacement function:

$$\mathbf{M} \ddot{\mathbf{r}}_n + \mathbf{C} \dot{\mathbf{r}}_n + \mathbf{K} \mathbf{r}_n = \mathbf{f}_n \quad (1)$$

where  $\mathbf{M}$ ,  $\mathbf{C}$  and  $\mathbf{K}$  are: the mass matrix, the damping matrix and the stiffness matrix, and  $\mathbf{r}_n$  is a displacement vector and  $\mathbf{f}_n$  - a global load vector at time  $t_n$ .

$$\dot{\mathbf{r}}_{n+1} = \dot{\mathbf{r}}_n + [(1-\delta)\ddot{\mathbf{r}}_n + \delta\ddot{\mathbf{r}}_n]\Delta t, \mathbf{r}_{n+1} = \mathbf{r}_n + \dot{\mathbf{r}}_n\Delta t + \left[ \left( \frac{1}{2} - \beta \right) \ddot{\mathbf{r}}_n + \beta\ddot{\mathbf{r}}_{n+1} \right] \Delta t^2 \quad (2)$$

where the parameters  $\beta$ ,  $\delta$  are determined by the direct integration is accuracy and stability. This method is conditionally stable, Clough and Penzien [4], for  $\beta=1/4$  and  $\delta=1/2$ , which corresponds to the assumption of the average constant acceleration in time.

After the substitution of eq. (2) to (1), the dynamic equation will be as follows:

$$(a_0\mathbf{M} + a_1\mathbf{C} + \mathbf{K})\mathbf{r}_{n+1} = \mathbf{F}_{n+1} + \mathbf{M}(a_2\dot{\mathbf{r}}_n + a_3\ddot{\mathbf{r}}_n) + \mathbf{C}(a_4\dot{\mathbf{r}}_n + a_5\ddot{\mathbf{r}}_n) \quad (3)$$

$$a_0 = \frac{1}{\beta\Delta t^2}, a_1 = \frac{\delta}{\beta\Delta t}, a_2 = \frac{1}{\beta\Delta t}, a_3 = \frac{1}{2\beta} - 1, a_4 = \frac{\delta}{\beta} - 1, a_5 = \frac{\Delta t}{2} \left( \frac{\delta}{\beta} - 2 \right) \quad (4)$$

### 3. FREE FALL LOADING OF TK-C30 CONTAINER

A hall crane transports the nuclear fuel in the TK - C30 steel container under a ceiling plate at +18.90 m. The cylinder container has a diameter of 2285 mm, a height of 4367 mm and a weight of 89.5 t. In the case of an accident the container can fall to the containment plate. The accident scenario was defined by a technological engineer in the paper Cesnak, J. and Králik, J. (2001).

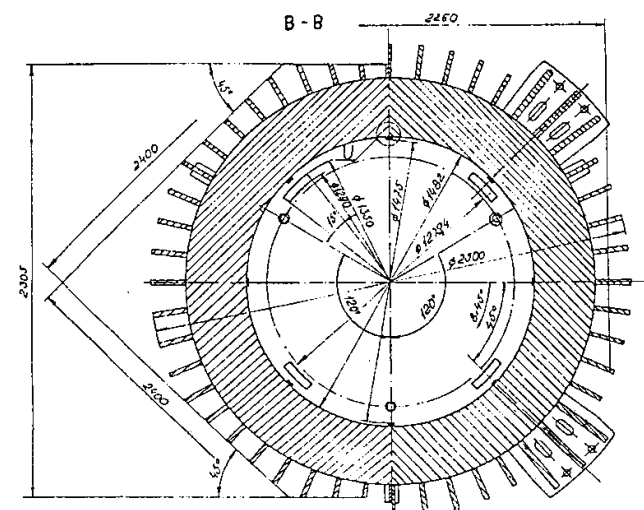
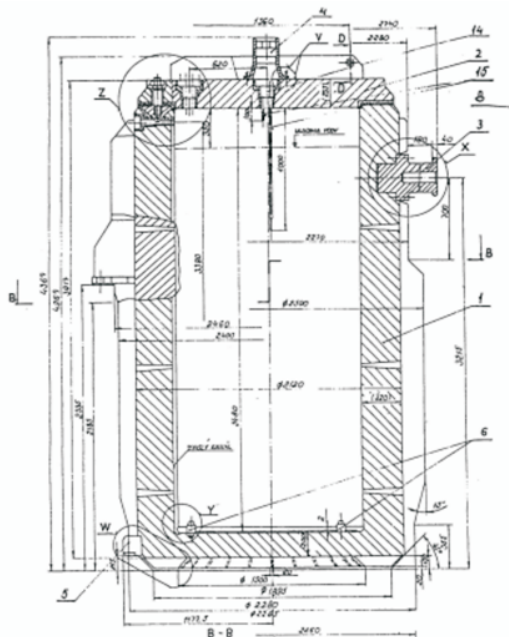


Fig. 4 Scheme of TK -C30 container.

Two possible tracks were defined (see Fig.5)

1. Track - at lines 31, 32, 33, 37, 38, 36, 39, 41
2. Track - at lines 31, 32, 33, 34, 35, 36, 39, 41

We proposed three levels of the container's fall:

1. Fall on the plate at level +18.90m from a height of 200 mm (points 31, 32, 33, 34, 35, 37, 38)
2. Fall on the plate at level +18.90m from a height 3670 mm (point 36)
3. Fall on the plate at level +7.30m from a height 15270 mm (point 41)

The impact loads can be defined from the equality of the kinetic energy  $E_k$  of the container's weight  $m_o$  before impact and the potential energy  $E_p$  of the plate's deformation at the moment of maximal impact effect

$$E_k = E_p \quad E_k = \frac{1}{2} m_o \dot{w}_o \quad E_p = \frac{1}{2} k w_{max} \quad (5)$$

where  $\dot{w}_o$  is the velocity of the container's fall at the moment of the plate-container contact;  $w_{max}$  is the maximal amplitude of the displacement of the plate,  $k$  is the stiffness of the plate (defined from the FEM model of structures). The velocity of the fall is

$$\dot{w}_o = \sqrt{2gh_o} \quad (6)$$

where  $h_o$  is the height of the free fall. The long time of the impact  $t_p$  and the amplitude of force  $F_{max}$  can be considered as the impact loads in the form of a half wave as follows :

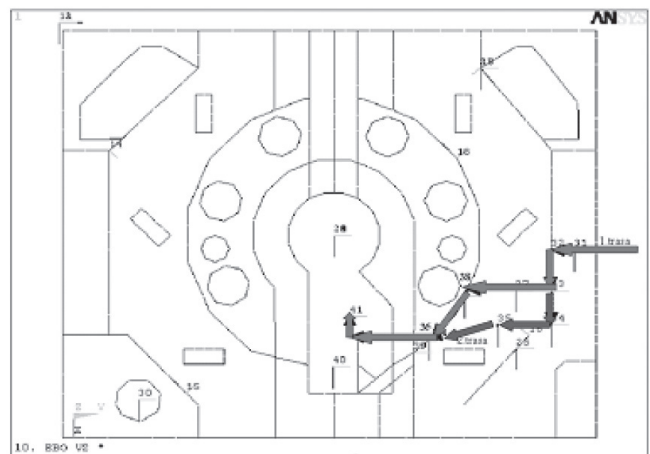


Fig. 5 The proposed method of the container's transport under a containment plate.



$$t_r = \pi \sqrt{\frac{m_o}{k}}, \quad F_{\max} = k \cdot w_o \sqrt{\frac{m_o}{k}} \quad (7)$$

The impact forces on the plate of the box SG at level +18.9m are presented in Table 1.

In the case of the fall of the container into the basin, we must consider two phases of the fall – firstly, the fall above a water surface ( $h_o$ ), and secondly, underwater ( $h_i$ ). Moreover, the kinematic energy of the fall on the basin bottom is

$$E_k = \frac{1}{2} m_o \dot{w}_1^2 - \frac{1}{2} m_o \dot{w}_o^2 \quad (8)$$

where  $\dot{w}_o$  is the velocity of the container's fall on the water surface (from the height  $h_o$ ), and  $\dot{w}_1$  is the velocity of the container fall on the basin's bottom.

The potential energy of the deformation is

$$E_p = \frac{1}{2} k w_{\max}^2 + m_o g h_v - \frac{1}{2} \rho A g h_k^2 - \rho A g h_k (h_v - h_k) \quad (9)$$

where  $w_{\max}$  is the maximum displacement due to the deformation of the structure on the basin's bottom due to the impact load;  $h_v$  (alias  $h_k$ ) is the height of the basin water (alias the container),  $A$  is the section area of the container,  $\rho$  is the density of the water,  $g$  is the gravitation acceleration.

The total time of the impact can be considered as a half wave from the equation of the vibration in the form

$$m_o \ddot{w}(t) + k w(t) + \rho g A w(t) = 0 \quad (10)$$

The fall of the container into a basin was tested by an experiment in the laboratory of CVUT Prague (Čihák and Medřický (1996)) in the case of a 1:10 experimental model. Based on the experimental results, the factor of the water resistance was equal to  $C_z=1.5$ .

The reaction force of the water resistance during the fall of the container is

$$F_z = \frac{1}{2} C_z A \rho \dot{w}_o^2, \quad (11)$$

where  $C_z$  is the factor of the water resistance defined by the experiment.

The velocity of the container's fall on the basin's bottom can be calculated from the equation

$$\frac{d}{dt} \dot{w} = \frac{(m_o - A z \rho) g}{m_o} - \frac{C_z A \rho \dot{w}_o^2}{2 m_o}, \quad (12)$$

The solution of (12) can be defined based on the experimental results in the form of an exponential function.

The velocity  $\dot{w}_i$  in the time step  $t_i = t_{i-1} + \Delta t$  and position  $z_i = z_{i-1} + \dot{w} \Delta t$  is expressed as follows

$$\dot{w}_i = \frac{1 + C_{ki}}{(1 - C_{ki}) n_1}, \quad C_{ki} = \left( \frac{n_1 \dot{w}_o - 1}{n_1 \dot{w}_o + 1} \right) e^{-2 n_1 n_2 t_i}, \quad (13)$$

$$n_1 = \sqrt{\frac{C_z A \rho}{m_o g}}, \quad n_2 = \frac{(m_o - A z_i \rho) g}{m_o}$$

The solution of the differential equation (12) using the difference approximation gives us the behavior of the position and velocity of the container's fall (Figure 6).

**Table 1** Impact loads from the container's fall.

Point (CSYS)	Height [mm]	Velocity [m/s]	Impact force [MN]	Period [s]
15119(CS31)	200	1.98	56.347	0.0093878
4143(CS32)	200	1.98	54.731	0.0096649
15156(CS33)	200	1.98	52.951	0.0099898
15165(CS34)	200	1.98	50.777	0.0104180
15382(CS35)	200	1.98	42.716	0.0123840
15335(CS37)	200	1.98	40.819	0.0129590
10826(CS38)	200	1.98	52.071	0.0101590
10064(CS39)	200	1.98	63.443	0.0083377
15535(CS40)	200	1.98	38.738	0.0136550
10827(CS36)	3670	8.14	277.65 (56.197)*	0.0081613
15498(CS41)	14010	15.31	583.07 (404.60)*	0.0007414

\* Impact force considering the damping effect of damping devices

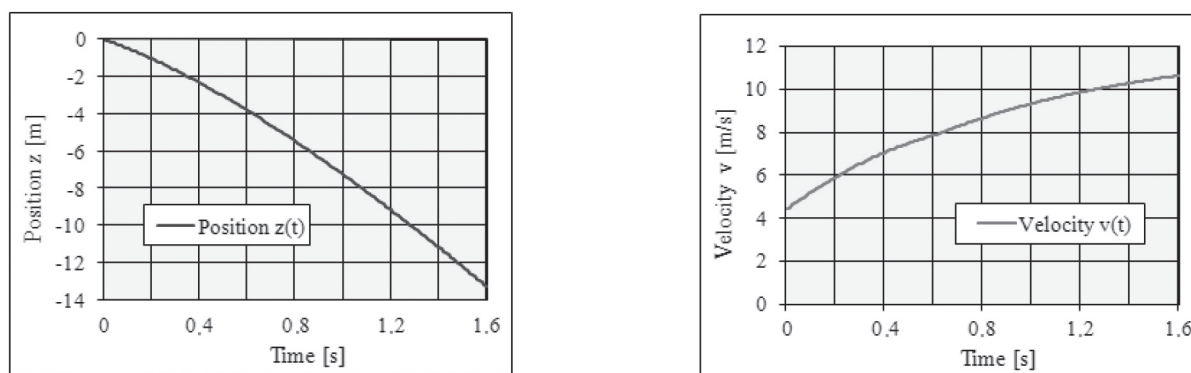


**Fig. 6** Position and velocity of container fall in the basin from the experiment of Čihák, F. and Medřický, V. (1996).

**Table 2**

Point (CSYS)	Height [mm]	Velocity [m/s]	Impact force [MN]	Period [s]
15498(CS41)	14010	15.31	583.07 (404.60)*	0.0007
15498(CS41)**	14010	10.70**	431.35 (358.23)*	0.0007

\*\* Calculation with water resistance,

\* Impact force considering the damping effect of damping devices

The impact forces on the plate of the SG box and the bottom of the basin, considering the water's resistance in the basin on the basis of the experimental results, are presented in Table 1. All the information about the impact loads – height, velocity, impact force and period are shown there.

If we calculate the water's resistance in the basin during the container's fall, the velocity of the movements of the container is diminished from a value of 15.31m/s to a value of 10.70m/s (see Table 2).

#### 4. SOIL -STRUCTURE INTERACTION

The dissipation of energy in the soil, as well as the soil deformation during the vibration of the structure, has the effect of total damping. It is possible to model the soil by finite elements or boundary elements as described by Králik, J. (2009). In the case of the loading of a power block building, caused by the container's falling and the continuous steam pressure, the boundary damping elements are accurate enough and thus create a realistic model.

The subsoil below the foundation plate was recently consolidated. The subsoil was characterized by layers of loess, loam and sand

gravel. Based on the geophysical reflex and refract research, the velocity of the longitudinal and transverse waves in the soil were found. For shear waves  $v_s = \sqrt{G/\rho}$  is valid where  $\rho$  is the soil density. Under the assumption that the foundation plate acts as a rigid body, the soil stiffness can be considered according to Barkan, D.D. (1948).

$$k_x = k_y = \frac{G}{1-\mu} \alpha_H \sqrt{ab}, \quad k_z = 2(1+\mu)G\alpha_V \sqrt{ab}, \quad (14)$$

where  $a$ ,  $b$ , are the foundation plate's width and length, and the coefficients  $\alpha_H$ ,  $\alpha_V$  can be determined according to Richart, F.E., Woods, R.D. and Hall, J.R. (1994),

$$\alpha_V = \frac{1-\mu}{4} \frac{m_b}{\rho r_a^3}, \quad \alpha_H = \frac{7-8\mu}{32(1-\mu)} \frac{m_b}{\rho r_a^3}, \quad (15)$$

where  $r_a = \sqrt{ab/\pi}$  is the equivalent foundation radius,  $m_b$  is the foundation's mass and  $\rho$  is the soil density.

#### 5. DAMPING MODEL

The damping of a vibration structure corresponds to the dissipation of mechanical energy, which is usually changed to thermal energy. In the case of reinforced concrete structures it is a viscous damping in the concrete in the uncracked compression zone and a damping due to friction between the reinforcement and concrete in the cracked tension zone. According to Clough, R., W., Penzien, J. (1993), IAEA (1996) in the case of an extreme load in reinforced concrete structures, it is possible to consider the damping ratio to the extent of 7-10% of the critical damping.

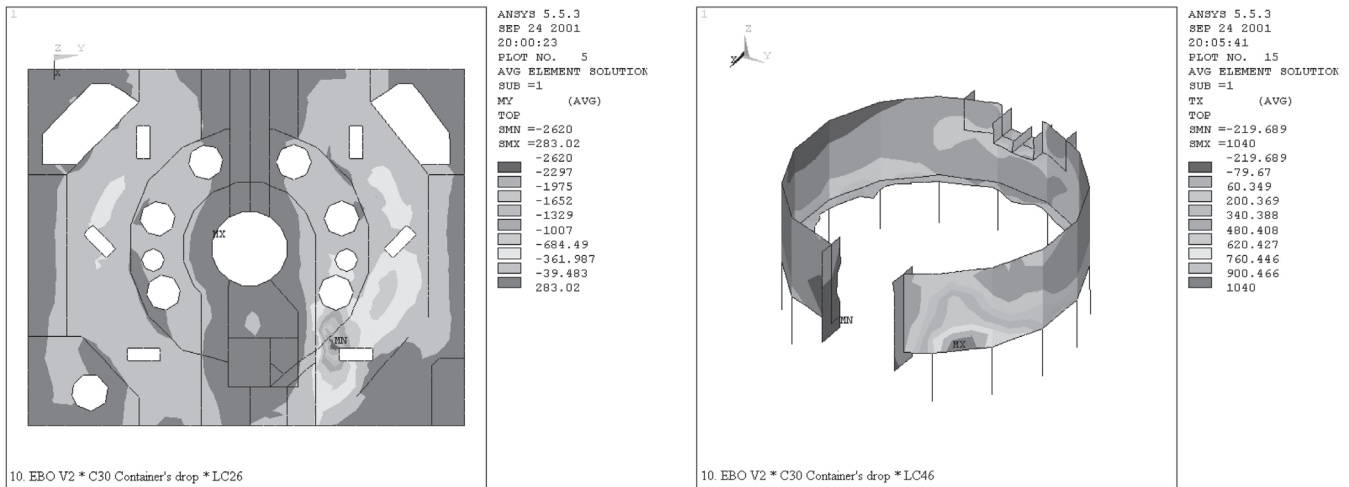


**Fig. 7** Envelope of bending moment  $m_y$  in a concrete plate at +18.9m and normal forces  $t_x$  in a circular wall.

The soil vibration is damped due to plastic deformation. The property of damping soil below the foundation plate is considered, according to Richart, F.E., Woods, R.D. and Hall, J.R. (1994), who have the value of

$$c_x = c_y = \frac{0,288}{\sqrt{\alpha_H}}, \quad c_y = \frac{0,425}{\sqrt{\alpha_V}} \quad (16)$$

In a linear analysis the Rayleigh damping model, which is proportional to the stiffness matrix, is used. The damping matrix in the dynamic equation (1) can be expressed as

$$\mathbf{C} = \alpha_o \mathbf{M} + \alpha_l \mathbf{K} \quad (17)$$

where the coefficient  $\alpha_o$ , ( $\alpha_l$ ) is decisive for the damping of lower (higher) natural frequencies. The Rayleigh damping coefficients can be determined from the solution of the conditional equation :

$$\begin{Bmatrix} \xi_m \\ \xi_n \end{Bmatrix} = \frac{1}{2} \begin{bmatrix} 1/ \omega_m & \omega_m \\ 1/ \omega_n & \omega_n \end{bmatrix} \begin{Bmatrix} \alpha_o \\ \alpha_l \end{Bmatrix} \quad (18)$$

where  $\omega_n$ ,  $\omega_m$  are the minimum and maximum natural frequencies from the structure's decisive natural frequencies, and  $\xi_n$ ,  $\xi_m$  are the values of the damping ratio of the critical damping.

As was shown, the damping ratio is different in a reinforced concrete structure, as well as in the soil and will be even more outstanding in a mechanical system's extremely loaded parts. The ANSYS system enables coverage of the true behavior of such a structure through the introduction of so-called material damping, which can be defined particularly for each element.

## 6. SOLUTION OF IMPACT RESPONSE

In the case of refueling during a reactor's shutdown, it is manipulated with 85t heavy containers above the reactor building's ceiling. If the suspension is released during this operation, the container can fall down on the ceiling or in the spent fuel storage pond, Bankash, M.Y.H. (1993).

For monitoring this situation in a complex structure, 3 different methods and 10 places in the ceiling structure and the basin bottom were chosen (see Cesnak, J., Králik, J. (2001)). During the modeling of the load the technical parameters from the operator were used.

The container's free fall was modeled as an impact load by Bankash, M.Y.H. (1993). The impulse intensity and its duration are expressed from the condition of the equality of the kinetic energy of a free falling body and the potential energy of the deformation of the load-bearing structure and container. The time interval of the impulse's action corresponds to 1/2 of the impulse period.

The response forces were calculated on the basis of the direct transient method in the ANSYS program. Thirteen load cases were considered in compliance with the impulses of force in tables 2 and 3. The envelope of forces were made from the time behavior. The envelope of the maximum intensity of the normal forces  $t_x$  [kN/bm] and bending moments  $m_y$  [kNm/bm] from the impact to the SG box ceiling are presented in Fig. 7. The peak of the bending moment in the concrete plate is near the point of the container's impact. In the case of a circular wall, the peak of the tension forces is on the bottom of the wall.

The envelope of the maximum intensity of the normal forces  $t_x$  [kN/bm] and bending moments  $m_x$  [kNm/bm] from the impact to the basin's bottom are presented in Fig. 8.

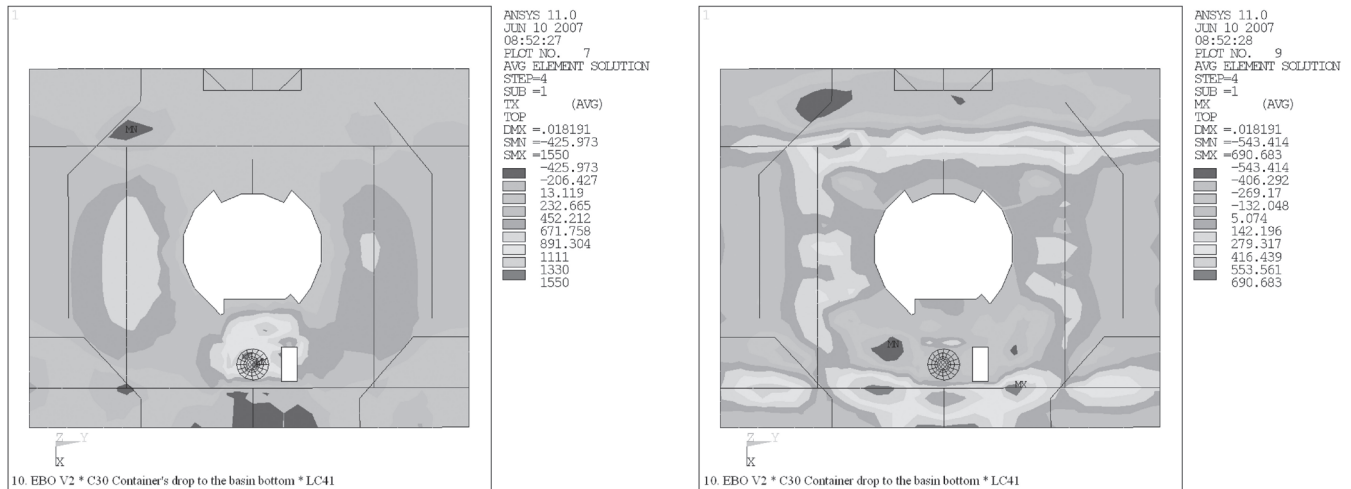


**Fig. 8** Envelope of maximum intensity of the normal forces  $t_x$  [kN/bm] and bending moments  $m_x$  [kNm/bm] from the impact to the basin bottom.

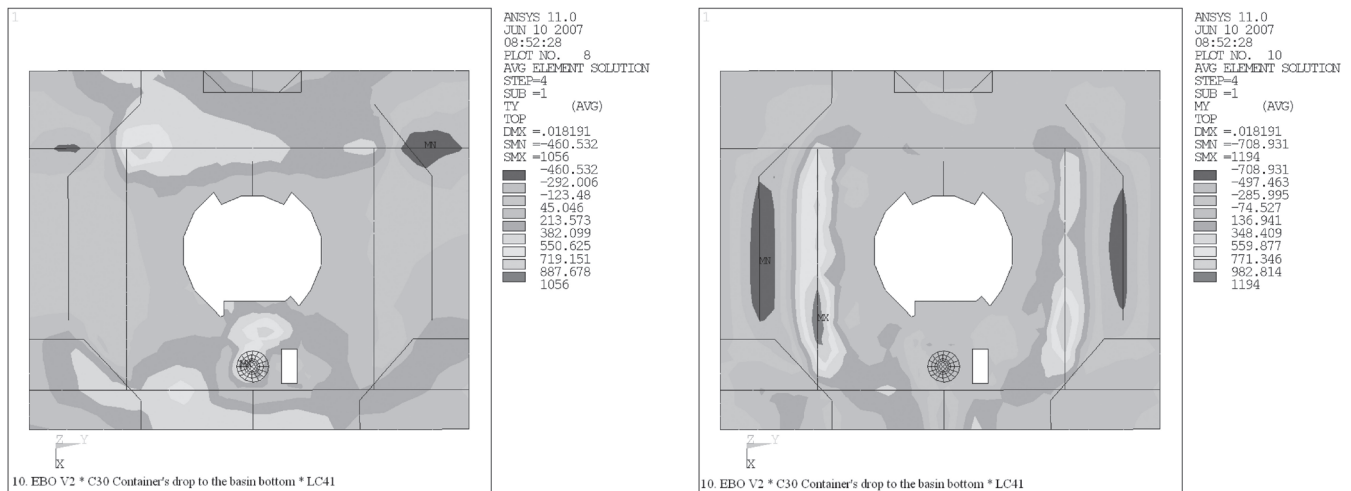


**Fig. 9** Envelope of maximum intensity of the normal forces  $t_y$  [kN/bm] and bending moments  $m_y$  [kNm/bm] from the impact to the basin bottom.

The envelope of the maximum intensity of the normal forces  $t_y$  [kN/bm] and bending moments  $m_y$  [kNm/bm] from the impact to the basin's bottom is demonstrated in Fig. 9. The peak of the tension forces in the concrete plate is near the point of the container's impact. The peak of the bending moments in the concrete plate is outside the point of the container's impact and along the walls. That is a consequence of the higher stiffness of the basin walls joined with the reinforced concrete reactor shaft (see Fig. 10). For example [3], in the case of a container falling from a height of 0.20m (3.67m), the speed at the moment of contact with the ground reaches

1.98m/s (8.14m/s), which corresponds to the impulse intensity 38.7-63.4MN (i.e. 277.6MN) in the period 0.008-0.014s (0.008s), depending on the stiffness of the reinforced plate at the point of impact. The maximum internal forces exceed the bearing capacity of the ceiling plate by about 6% due to the impulse intensity 277.6MN in the time impulse 0.008s. In the case of falling from a height 1.0m above a water surface in a basin, the intensity impulse is equal to 583.07MN (i.e. 431.35MN) in the period 0.007s. The bearing capacity of the basin bottom is equal to 99.91%. The second effect of a container's fall in the case of a crane accident





Two types of damping devices (Tab.5) were considered. Two of them (type – T1) are designed in one pipe layer; the rest (type – T2) are designed in two pipe layers.

The proposed damping devices are from short pipe elements mutually connected with the steel beams from the U-profile in

a grid form (Fig. 13). The detail of the type T2 damping device is presented in Fig. 14.

This pipe element was tested by Bundesanstalt für Materialprüfung (see Table 5) for the plastic capacity of the device due to the impact load. The safe crosswise deformation of the pipe element was defined on the basis of the experimental results as  $0.85D_s$  (Fig. 15).

The plastic capacity of the pipe device (Fig.15) is defined as follows

$$F_m = 2\alpha \sigma_F b d^2 / (D_s - a) \quad , \quad (24)$$

where  $\alpha$  is the reliability parameter ( $\alpha = 1.1$ ),  $\sigma_F$  - stress yield ( $\sigma_F = 350\text{MPa}$ ),  $b$  - length of pipe,  $d$  - thickness of pipe,  $D_s$  - diameter of pipe,  $a$  - height. The maximal plastic deformation of a pipe that can be used is  $0.85D_s$  and the maximal diameter dilatation is  $a = 1.5D_s$ . Three layer damping devices from  $2 \times 24 \times 219/20 - 150\text{mm}$  pipes were proposed to dissipate the kinetic energy  $E_k = 2702.5\text{kNm}$  (free fall from height of  $3670\text{mm}$ ) with an efficiency of  $\eta = 107.9\%$ . In the case of a basin bottom an effective damping device is designed as  $2 \times 52 \times 219/18 - 150\text{mm}$ , which dissipates the kinetic energy  $E_k = 5120.0\text{kNm}$  (free fall from height  $14010\text{mm}$ ) with an efficiency of  $\eta = 110.2\%$ .

**DETAIL Y**

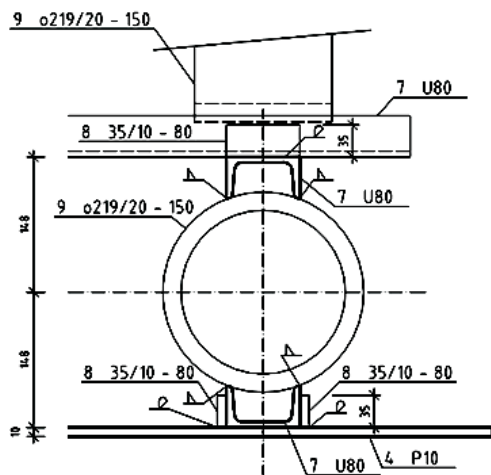


Fig. 14 Detail of pipe damper.

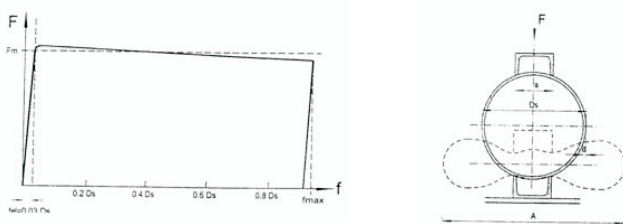


Fig. 15 Experimental test of the pipe's resistance.

**8. PROBABILITY AND SENSITIVITY ANALYSIS OF DAMPING DEVICE**

The methodology for the probabilistic analysis of the efficiency of a damping device results from the requirements [9, 16] and experience gained from their applications. In this case the MONTE CARLO direct simulation method by Marek, P., Brozzetti, J. and Guštar, M. (2001) to solve the reliability of damping devices was used. The probability of the loss capacities in the case of the plasticity deformation of steel pipes under the container's impact will hence be calculated from the probability of the no accomplishment condition of reliability  $RF$ ,

Table 4 Comparison of effectivity of a damping devices.

Type	Diameter of pipe	$E_k$ [kJNm]	$E_p$ [kJNm]	$\eta$ [%]
Free fall from height <b>3.670mm</b>				
T1	1 x 18 x 219/18 - 455mm	2962.4	2688.0	90.7
T2	2 x 24 x 219/20 - 150mm	2702.5	2917.4	107.9
Free fall from height <b>14.010mm</b>				
T3	1x 24 x 219/22 - 380mm	4753.2	4471.4	94.1
T4	2x 52 x 219/18 - 150mm	4644.4	5120.0	110.2

**Table 5** Experimental test of a pipe segment (*Bundesanstalt für Materialprüfung*).

Specimen No.	Drop in mm	Deformation in mm	Potential Energy <sup>1)</sup> in Joule	Velocity Fall <sup>2)</sup> in m/s	Deformation Energy in Joule	Load Impulse over 30ms in kN
1	1400	68	10369	5.2	9880	108
2	1600	82	11880	5.6	11300	107
3	1700	72	12516	5.8	11900	110
4	1800	90	13350	5.9	12700	106

1) This energy corresponds to the drop plus the pipe's deformation calculated from the permissible pipe crack

2) This value corresponds to the velocity of the test frame at the moment of contact with pipe

$$P_f = P(RF < 0), \quad (25)$$

where the reliability condition is defined in the form

$$RF = E_p - E_k \geq 0, \text{ various in the form relative } RF = E_p / E_k - 1 \geq 0 \quad (26)$$

where  $E_p$  is the potential energy of the plasticity capacity of the structure,  $E_k$  the kinetic energies of the impact load.

The probability of failure can be defined by the simple expression

$$P_f = P[E_p < E_k] = P[(E_p - E_k) < 0] \quad (27)$$

The reliability function  $RF$  can be expressed generally as a function of the stochastic parameters  $X_1, X_2$  to  $X_n$ , used in the calculation of  $R$  and  $E$ .

$$RF = g(X_1, X_2, \dots, X_n) \quad (28)$$

The failure function  $g(\{X\})$  represents the condition (reserve) of the reliability, which can either be an explicit or implicit function of the stochastic parameters and can be single (defined on one cross-section) or complex (defined on several cross-sections, e.g., on a complex finite element model).

The failure surface or limited state can be defined as  $g(\{X\}) = 0$ , which is the boundary between the safe and unsafe region. The failure probability may be calculated as

$$P_f = \iiint \dots \iint_{g(X) < 0} f_X(X_1, \dots, X_n) dX_1 \dots dX_n \quad (29)$$

where  $f_X(X_1, \dots, X_n)$  is the joint probability density function of the multivariable  $\{X\}$ . The multi-dimensional integration over the failure region should be performed to calculate  $P_f$  in Equation (29). This requires information concerning the joint probability density function  $f_X(X_1, \dots, X_n)$ . In general, this information is often

unavailable or practically impossible to obtain. Performing the multidimensional integration could be extremely difficult to achieve. Therefore, approximate approaches to perform this integration are required to evaluate the probability of failure.

In the case of simulation methods the failure probability is calculated from an evaluation of the statistical parameters and theoretical model of the probability distribution of the reliability function  $g(X)$ . The failure probability is defined as the best estimation on the basis of numerical simulations in the form

$$p_f = \frac{1}{N} \sum_{i=1}^N I[g(X_i) \leq 0] \quad (30)$$

where  $N$  is the number of simulations,  $g(\cdot)$  is the failure function, and  $I[\cdot]$  is the function with a value of 1, if the condition in the square bracket is fulfilled; otherwise, it is equal to 0.

The variation of the failure function can be defined by Melcher in the form

$$s_{p_f}^2 = \frac{1}{(N-1)} \left\{ \frac{1}{N} \left[ \sum_{i=1}^N I^2[g(X_i) \leq 0] \right] - \left[ \frac{1}{N} \sum_{i=1}^N I[g(X_i) \leq 0] \right]^2 \right\} \quad (31)$$

The various forms of analyses (statistical analysis, sensitivity analysis, probabilistic analysis) can be performed. Most of these methods are based on the integration of MONTE CARLO (MC) simulations. The accuracy of this method depends on the number of simulations and is defined by the variation coefficient

$$v_{p_f} = \frac{1}{\sqrt{N p_f}} \quad (32)$$

where  $N$  is the number of simulations. When the target probability of failure is  $p_f = 10^{-4}$ , the variation factor is equal to 10% for the number of simulations  $N=10^6$ , which is acceptable.

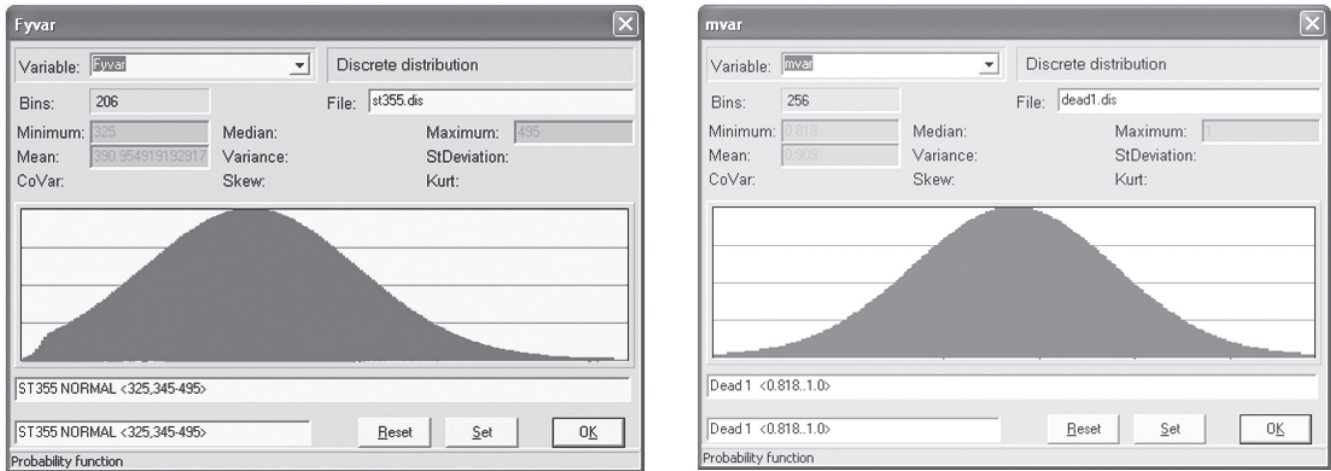


Fig. 16 Histogram of input parameters – a) Design strength of steel b) Container mass.

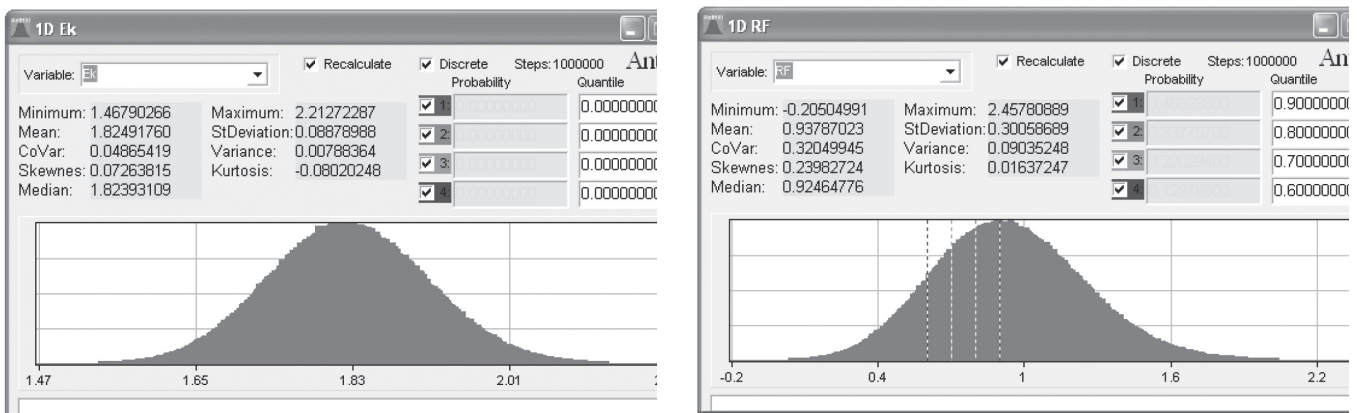


Fig. 17 Histogram of output parameters for T1 – a) Kinematic energy  $E_k$  b) Reliability function RF.

The failure probability for the case of a single limit state function can be extended directly to that for series and parallel systems. For example, the indicator function in Equations (30) for a series system becomes

$$I\left[\bigcup_{i=1}^n g_i(x) < 0\right] = \begin{cases} 1 & \text{if } I[.] \text{ is true} \\ 0 & \text{otherwise} \end{cases} \quad (33)$$

The difference in the importance of the application of the sampling technique in this case is that the presence of numerous limit state functions complicates the choice of  $h_x(x)$ . A simple solution is to consider the multimodal sampling function given by

$$h_x(x) = \sum_{i=1}^N w_i h_{x_i}(x) \quad \text{where} \quad \sum_{i=1}^N w_i = 1 \quad (34)$$

and  $h_{x_i}(x)$  is the sampling distribution determined, based on the  $i^{\text{th}}$  limit state function, and  $w_i$  is the weight, which is inversely proportional to  $\varphi_i$ .

The probabilistic analysis of the damping device's reliability to absorb the kinetic energies of the container fall was realized by a simulation of the design check using the MONTE CARLO direct method under the AnthILL system (Marek, P., Brozzetti, J. and Guštar, M. - 2001) and ANSYS (Králík, J. - 2009).

**Table 6** Parameters for the random variable.

Variable	Character. value	Variable coefficient	Bounded histogram	Mean value	Standard deviation
Fy - design strength of steel [MPa]	392	Fy.var	ST355	1	0.07
m – container mass [t]	89.5	mvar	DEAD1	0.909	0.04
h - fall distance [m]	3.67/14.01	hvar	N1-10	1	0.033
hn – depth of basin [m]	13.01	hn.var	N1-10	1	0.033
D – diameter of pipe [mm]	219	Dvar	N1-01	1	0.0033
b - length of pipe [mm]	455/150 380/150	bvar	N1-10	1	0.033
t – thickness of pipe [mm]	18/24 24/52	tvar	N1-10	1	0.033
c – width of U beam + plate [mm]	77	cvar	N1-05	1	0.017
a – height of U beam [mm]	80	avar	N1-05	1	0.017
S – area of container [m2]	4.10	Svar	N1-10	1	0.033
hk– height of container [mm]	4367	hk.var	N1-05	1	0.017

**Table 6** Parameters for the random variable.

Affectivity of damping in %	$P_f$ - Probability of the damping device failure		
	T1	T2	T4
60	0.0	0.0	0.0
70	0.000089	0.0	0.0
80	0.007303	0.000032	0.0
90	0.083356	0.002333	0.000006
100	0.320213	0.030070	0.000708

The probabilistic analysis of an accident due to the means of transport of a container above a containment plate results from uncertainty as to the material and geometry properties, load level, non-linear deformation and design condition.

On the basis of the mentioned inaccuracy of the input data for a probabilistic analysis of the loss damping capacities of the steel pipes, their mean values, standard deviations and variable constant for normal distribution were determined. The discrete histograms of the AntHILL program were used (Table 5). The histograms of input parameters – the design strength of the steel and container mass are presented in Fig.16. The histograms of the output parameters – the kinematic energy  $E_k$  and reliability function  $RF$  after the  $10^6$  MONTE CARLO simulation are presented in Fig.17.

The calculation of the impact response and sensitivity analysis of the damping device's effectivity was considered in the ANSYS program.

Three types of damping devices with various geometries of steel pipes in one and two layers were analyzed (Table 6). The damping devices (types T1 and T2) were designed for the free fall of

a container on a containment plate. Type T1 is satisfying in the case of 70% effectiveness of damping the impulse, T2 for 80% effectiveness. The damping devices (type T4) were designed for the free fall of a container on a basin's bottom. Type T4 is satisfying in the case of 90% effectiveness of damping the impulse.

The sensitivity analysis of the damping devices was realized in the ANSYS program. The results from this analysis show that the effectiveness of the damping devices depends firstly on the material properties of the steel – the strength and thickness of the pipes; secondly, on the variability of the container mass and the height of the free fall (Fig.18). The ratio of the influence of these input parameters are different in the T1 (Fig.18a) and T4 (Fig.18b) damping devices.

## 9. CONCLUSION

This paper deals with the problem of the analysis of buildings of nuclear power plants in the case of their resistance to a possible accident during the transport of a TK C30 container (Cesnak, J., Králik, J. -2001) with nuclear fuel. Depending on the importance of these buildings, not only numeric analysis, but also experimental measurement (Čihák, F. and Medřický, V. -1996) were provided.

The dynamic transient analyses from the container's drop during the accident simulation were realized using the ANSYS system. During a container's drop simulation the influence of the load-bearing structure's vibration is very significant for the bearing capacity of the steam generator suspensions, which are anchored in the ceiling. During the reconstruction of the containment structure damping

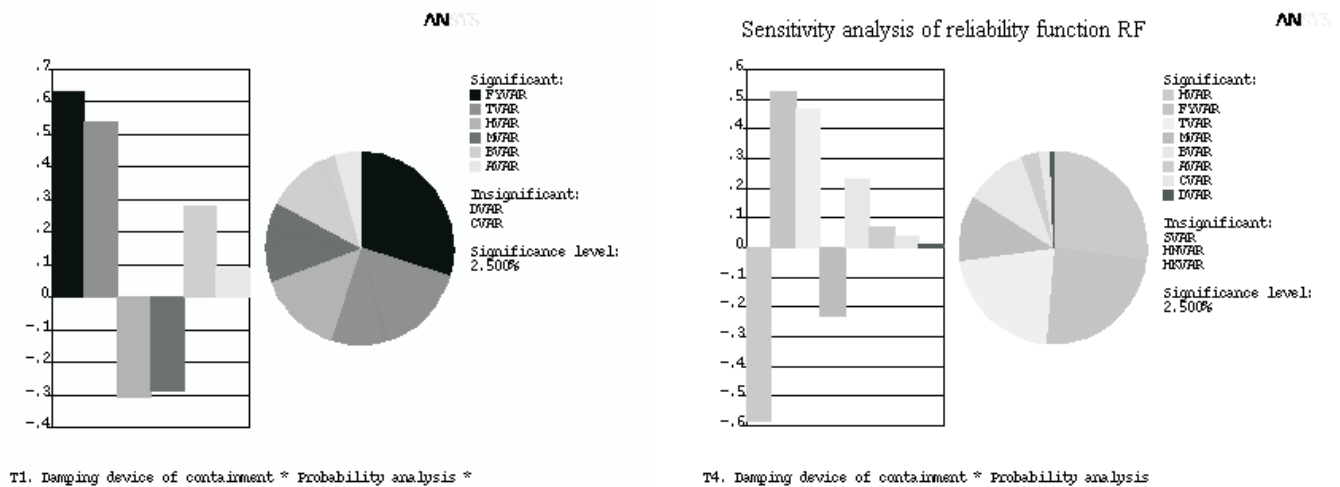


Fig. 18 a, b Sensitivity analysis of the reliability of T1 and T4 damping devices.

devices from steel pipes were designed. The flooring plate of the containment was protected from the container drop by reducing the effect of the impact using the damping devices from the pipe elements.

The damping devices were designed in accordance with the results of tests of Bundesanstalt für Materialprüfung. The kinetic energy was dissipated in the plastic deformation of the steel tubes.

The probability and sensitivity analysis of the effectiveness of the damping devices were realized by the ANTHILL and ANSYS programs.

The uncertainties of the load levels (container mass, height of free fall), the geometric and material properties (steel strength, geometric characteristic of pipe segments) and other influences

following the inaccuracy of the calculated model and numerical methods were taken into account in the  $10^6$  direct MONTE CARLO simulations. In accordance with the probability and sensitivity analysis, the reconstruction project of the protection of the NPP building before a crane accident due to transport of the TK C30 container was proposed.

## ACKNOWLEDGEMENT

The project was realized with the financial support of the Grant Agency of the Slovak Republic (VEGA). The project registration number is VEGA 1/0849/08 and 1/4197/07.

**REFERENCES**

- [1] **Bankash, M., Y., H. (1993)** *Impact And Explosion. Analysis and Design*. Oxford, London
- [2] **Barkan, D., D. (1948)** *Dynamic of Soil and Foundation*, Gosstrojizdat, Moskow (in Russian)
- [3] **Cesnak, J. and Králik, J. (2001)** *Reliability Analysis of the Reinforced Concrete Structures of Containment under Transport Way of Container C30*. Obj.800 JE-V2, PRO-REK, Bratislava
- [4] **Clough, R., W. and Penzien, J. (1993)** *Dynamics of structures*, McGraw-Hill, Inc.
- [5] **Čihák, F. and Medřický, V. (1996)** *Drop of Container Castor 440/84 in Water Tank ŠI-Cylinder Water Tank*. 1996, CVUT Prague, FSV, 40 pp. (in Czech)
- [6] **Eurocod 2 (1992)** *Design of Concrete Structures - Part 1-1 General Rules and Rules for Buildings ENV1992*, CEN
- [7] **IAEA (1996)** *Technical Report, Guidelines for WWER 440/213 Containment Evaluation*, IAEA/TA-2488, RER/9/035, WWER-SC-170, Vienna
- [8] **Janas, P. and Krejsa, M. (2002)** Numerical Probabilistic Calculation With Cut Off Histograms, *3<sup>rd</sup> International Conference, Reliability of Structures*, p.33-38.
- [9] **Jcss-Ostl/Dia/Vrou-10-11-2000 (2001)** *Probabilistic Model Code, Part 1 Basis of Design*, Working Material, <http://www.jcss.Ethz.Ch/>.
- [10] **Kanický, V. and Salajka, V. (1994)** Some Remarks on the Application of Professional Fem-Based Programs. In: *Numerical Methods in Continuum Mechanics, Proceedings of the International Scientific Conference*, September 19-22, High Tatras, Stará Lesná - Slovakia, pp. 345-352.
- [11] **Kotrasová, K. (2008)** Influence of Height of Filling and Category of Sub-Soil for Liquid Storage Cylindrical Tanks, In: *Selected Scientific Papers, Journal of Civil Engineering*, TU Košice, Vol.3, Issue 1.
- [12] **Králik, J. and Cesnak, J. (1995)** Impact and Explosion Analysis of Nuclear Power Plant Building. In proc. of *International RILEM Conference on Dynamic Behavior of Concrete Structures*, September, Expertcentrum TU Košice.
- [13] **Králik, J. and Cesnak, J. (2006)** Experimental and numerical reliability analysis of damping devices under impact loads from container. In: *First European Conference on Earthquake Engineering and Seismology*. Abstract Book. 3-8 September, Geneva, Switzerland. pp. 256.
- [14] **Králik, J. (2009)** *Safety and Reliability of Nuclear Power Buildings in Slovakia. Earthquake – Impact - Explosion*. Ed. STU Bratislava, 307 pp.
- [15] **Malý, J., Štěpán, J., Schererová, K. and Holub, I. (2003)** Calculation of Floor Concrete Structure Loaded by a Container Drop. In *Procs. 17<sup>th</sup> International Conference on Structural Mechanics in Reactor Technology, SMIRT 17*, Prague, CR, August 17-22.
- [16] **Marek, P., Brozzetti, J. and Guštar, M. (2001)** *Probabilistic Assessment of Structures Using Monte Carlo Simulation, Background, Exercises and Software*, ITAM Academy of Sciences of Czech Republic, Glos S.R.O., Semily, Czech Republic, Prague.
- [17] **Melcer, J. and Marčoková, M. (1996)** Some Considerations on the Creation of Computing Models. *Studies of University of Transport and Communications In Žilina, Civil Engineering Series*, Vol. 20, Editing Centre, VŠDS, Žilina, pp.73-90.
- [18] **Plocek, Z., Štěpánek, P., Salajka, V., Kala, J. and Kanický, V. (2007)** Design of Earthquake Resistance Enhancements of the Dukovany Nuclear Power Plant Building Structures, In *Procs. Second international symposium on Nuclear Power Plant Life Management*, 15–18 October, Shanghai, China.
- [19] **Richart, F., E., Woods, R., D. and Hall, J., R. (1994)** *Vibrations of Soils and Foundations*, Prentice-Hall, Englewood Cliffs.
- [20] **Řeřicha, P. and Šejnoha, J. (2004)** Prediction of the Lifetime of NPP Containment Considering Various Accidents. In: *Reliability of the Structures*, Ostrava: Dům Techniky, pp. 7-10.
- [21] **Žmindák, M., Sapietová, A. and Klimko, J. (2008)** Modeling of Damping in Finite Element Method. In: *6<sup>th</sup> International Conference on “Dynamics of rigid and deformable bodies 2008”*, September 17-19, Ústí nad Labem, CR, University of J.E.Purkyně, Ústí n.L., pp. 201-208, (in Slovak).